Cellulose fiber as bacteria-carrier in mortar: Self-healing quantification using UPV

Harshbab Singh & Rishi Gupta

March 2020

Cellulose fiber as bacteria-carrier in mortar: self-healing quantification using UPV

Harshbab Singh[1] and Rishi Gupta[2,*]

[1] Department of Civil Engineering, University of Victoria, 3800 Finnerty Road, Victoria, B.C, V8P 5C2, Canada; harshbabsingh@uvic.ca

[2] Engineering and Computer Science (ECS), 314, Department of Civil Engineering, University of Victoria, 3800 Finnerty Road, Victoria, B.C, V8P 5C2, Canada.

[*] Correspondence: guptar@uvic.ca

Abstract:

Crack formation due to shrinkage or tensile forces is a major weakness of cementitious materials. To overcome this problem, in this study a self-healing mortar is produced using mineral producing alkaliphilic bacteria. Authors have used *bacilius subtilis strain 168 type* of bacteria to improve the ability of cementitious mortar to heal any formed cracks without any external intervention. Bacteria-based self-healing concrete/mortar needs bacteria-carriers to protect bacteria in a dense matrix to maintain the mineral-forming capacity of bacteria. However, the currently used bacteria-carriers are not always suitable for concrete because of their complex procedures or high cost. To develop a more suitable bacteria-carrier, in this paper feasibility of alkali treated micro cellulose fiber as a novel bacteria-carrier for self-healing mortar is investigated. Two types of bacterial mortar by using cellulose fiber as a bacteria-carrier were prepared. For one type, nutrients were added inside the mortar mix, while for the other, nutrients were added into the curing water. The crack healing efficiency of bacterial mortars was investigated using image analysis and ultrasonic pulse velocity (UPV) test and compared with unreinforced and control cellulose fiber mortars. Research shows that self-healing mortar using cellulose fiber as a bacteria-carrier result in maximum self-healing as compared to other mixes, 8.23% more than control samples, pre-cracked at 28 days with damaged degree between 0.1 to 0.2. At the dosage investigated, addition of cellulose fiber resulted in a decrease in compressive strength. It was observed that cellulose fiber increase the availability of bacteria in cracked region by acting as a bridge across the crack. Furthermore, cellulose fibers have a low cost and simplest method of immobilizing bacteria when compared with other bacteria carriers.

Keywords: self-healing mortar; bacteria-carrier; cellulose fibers; ultrasonic pulse velocity; cracks

1. Introduction:

Cement/concrete is still one of the widely used materials in the construction industry. One downside, however, is that cement production alone contributes around 7% to global anthropogenic CO2 emissions [1] and exerts negative impacts on the environment. Traditional concrete has another drawback, it tends to crack when subjected to tensile stresses. Cracking leads to an increase in permeability, decrease in durability and strength of the concrete structure. Due to the increase in permeability, the water easily passes through the concrete matrix and comes in the contact with the reinforcement leading to corrosion initiation. Due to this, the strength of the concrete structure decreases, necessitating repair of cracks [2]. Conventional repair methods use manual inspection followed by filling of cracks with cement or other synthetic fillers [1], which are very expensive and time-consuming. It is estimated that in Europe, cost related to repair works is half of the annual construction budget [3]. Therefore, to date the various self-healing repair methods including adhesive based, autogenous, mineral admixture based and bacteria-based are developed to heal the cracks automatically without any external source [4, 5], and are helpful in decreasing the operational cost as compared to manual methods. Bacteria-based self-healing has become more popular recently because it has a better healing capacity and uses commonly available environment-friendly microbes.

Bacteria-based self-healing works on the phenomenon of microbiologically induced calcite precipitation (MICP). A mineral producing alkaliphilic bacteria with calcium-based nutrients in cement mortar helps in precipitation of calcium carbonate caused by metabolic activities of microbes. The precipitation of calcium carbonate helps to heal the cracks in cement mortar, resulting in an increase of the overall durability of the material. The MICP is feasible by two metabolic activities of bacteria, hydrolysis of urea [6] and working of bacteria on calcium-based nutrients [1]. In the former process, urea is used as a nutrient and results in the production of two ammonium ion for each carbonate ion during the formation of calcium carbonate, which results in the additional nitrogen loading and has a negative effect on the environment [1]. While in the latter case, the carbon dioxide is consumed and results in additional production of calcium carbonate. The advantage of this process when calcium lactate is used as a nutrient is that it does not have any impact on the setting time of concrete [7].

A carrier is required to protect the bacteria from mechanical forces caused by mixing processes and hydration reaction in the cement matrix. Basically, methods to immobilize bacteria can be divided into two categories, encapsulated and adsorbed depending upon the technique of immobilization, see Table 1.

In the encapsulated method, bacteria and nutrients are immobilized in micro or macro-capsules, spherical or cylindrical in shape. When crack hits these capsules, results in rupturing of the capsules and the bacteria and nutrients are released out, and precipitation takes place to heal the cracks [11]. However, the probability of crack hitting the capsule is very low due to a limited number of capsules available in the crack region, especially for spherical capsule because they have less bond strength with the concrete matrix. On the other hand, cylindrical capsules have more bond strength with concrete, but they cause less release of nutrients due to the suction effect on the sealed end [15]. Microcapsules are mainly manufactured using bulk emulsification polymerization techniques, but these methods have concerns related to capsule dimensions and bonding with the concrete matrix [16]. Also, these techniques required advanced equipment and complex procedures.

In the adsorbed method, bacteria and nutrients are immobilized in a porous material with high porosity by saturating the material with bacterial suspension. The highly porous material is helpful in providing enough space for bacteria growth, oxygen, and water, essential for MICP.

Table 1. Bacteria-carriers used in different researches

Immobilization category	Bacteria carrier	Immobilization technique	Self-healing performance
Adsorbed	Expanded Perlite (EP) [8]	Impregnated under vacuum, drying in an oven, coating with a geopolymer.	Completely healed crack width up to 0.79 mm after 28 days of healing
	Expanded Clay Pellets (EC) [9]	Impregnated under vacuum and drying in an oven	Completely healed crack width up to 0.46 mm after 100 days of healing
	Ceramsite [10]	Alkali erosion and sintering treatments, heat treatment at 750° C, soaking and drying in an oven	Maximum crack width healed 0.3mm
Encapsulated	Epoxy [11]	Preparation of microcapsules by using in-situ polymerization procedure	Maximum crack healing 45% for crack size of 0.1 mm healed at 50º C.
	Hydrogel [12]	Mixing of spores with the polymer solution, addition of initiator, UV irradiation for 1 hour, freeze grinding and drying.	Maximum crack width healed 0.5 mm after 28 days.
	Melamine [13]	Preparation of microcapsules using a polycondensation reaction	Maximum crack width healed 0.97 mm.
	Polyurethane [14]	Mixing of spores with a two-component polyurethane to form PU foam	60% regain in the strength of cracked mortar specimen.

To date, various carriers have been adopted like polyurethane [14], melamine [13], silica gel [14], expanded clay particles [7, 9], lightweight aggregates [17], graphite nano platelets [17], perlite [8], diatomaceous earth [18], and ceramsite [10]. The complication and relatively high cost of immobilization methods have made them impractical to use on a large scale in the construction industry.

So far, the most suitable carrier for bacteria has not been found, creating the need to develop better techniques to carry bacteria. In this study, the feasibility of using cellulose fiber as a carrier for bacteria is investigated.

Van Tittelboom and Belie [15] explained in their study, self-healing in concrete is more effective when the crack width is restricted (Figure 1(a)), water is available in the cracks (Figure 1(b)), and crystallization (Figure 1(c)).

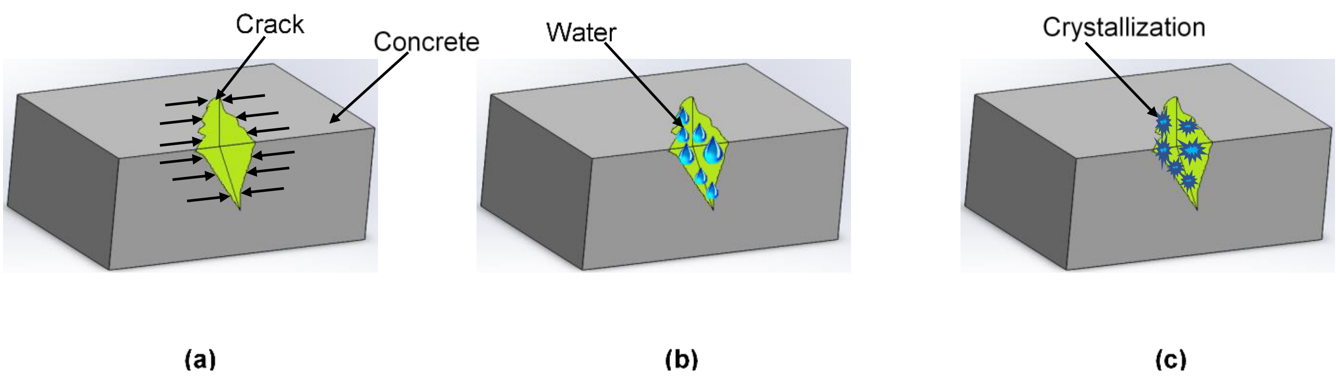

Figure 1. Conditions to improve self-healing: (a) Restriction of crack width; (b) Availability of water; (c) Crystallization. (Concept adopted from Van Tittleboom and Belie [15])

Authors hypothesize that cellulose fiber can assist in improving all three mechanisms. For (**a**), cellulose fibers can limit crack width in plastic shrinkage phase [19] and can reduce the cracking by 85% more than normal concrete [20, 21]. (**b**), cellulose fibers have a high water absorption of 85% [22], thus improving internal curing and assisting in mechanism (**b**). Finally, since cellulose fibers have high alkali resistance [23], they can protect bacteria from highly alkaline concrete environment and would provide enriched sites for bacteria to MICP.

The working mechanism of cellulose fiber based bacterial mortar is shown in Figure 2. When the mortar is not cracked the bacteria remain dormant inside the fibers distributed throughout the matrix. After the cracks appeared, the cellulose fibers containing bacteria act as a bridge between the crack surfaces, outside oxygen and water can enter the mortar through cracks, activating the bacteria. The activated bacteria work on the nutrients present in the mortar or in curing water and results in the MICP to seal the cracks gradually.

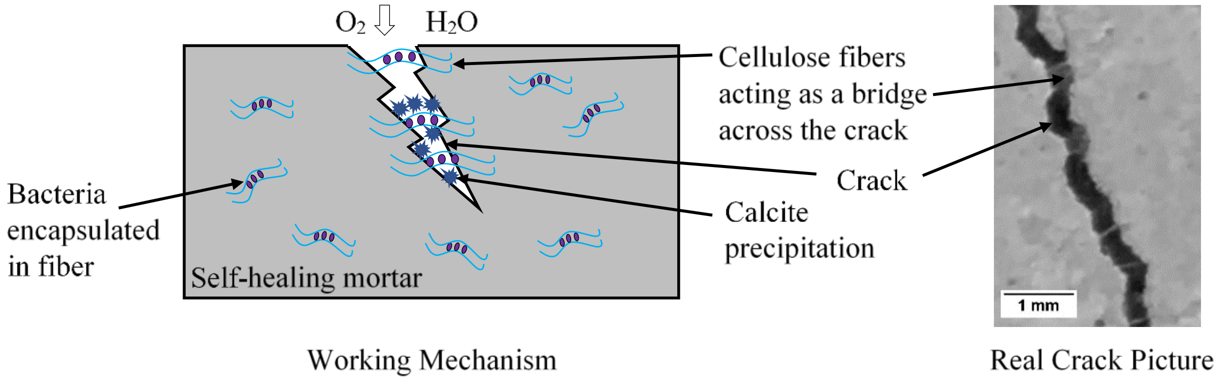

Figure 2. The working mechanism of self-healing mortar using cellulose fiber as a bacteria-carrier.

In self-healing mortar the advantages of using cellulose fiber are:

- The high porosity of fibers helps to provide space for the growth of bacteria, in addition, the porosity of fiber helps to absorb water and oxygen, which can be utilized by bacteria at the time of MICP.
- Fibers work as a bridge across the crack surfaces, resulting in an increase in the availability of bacteria for the self-healing inside the crack.
- Fibers help to reduce brittleness and the microcracking in the mortar leads to an increase in the efficiency of self-healing.
- Immobilization of bacteria can be done by just submerging fibers into bacterial suspension to make them saturate, which is a very easy and practical method.
- Cellulose fibers are also suitable for concrete ready-mix plants [21], making them easy to use as a bacteria-carrier for the small to large scale concrete structures.

Cellulose fiber also improves the internal bonding, modulus of rupture and elasticity of cement composites [24]. In addition, cellulose fibers in concrete increase the freeze-thaw durability [25] and provide a nice finished surface [26]. So, it is hypothesized that the use of cellulose fiber as a bacteria-carrier would resist the crack formation as well as improve the self-healing of the cement mortar. In this investigation, the crack healing efficiency and change in compressive strength for different types of cement mortar containing bacteria absorbed in cellulose fiber have been evaluated.

2. Experimental Program:

2.1 Material Properties:

The following sections specify the types and associated properties of different materials used in the preparation of cement mortar:

2.1.1. Cement

General use Type GU Ordinary Portland Cement (OPC), which meets the requirements of type-I and type-II cement as per ASTM C150 [27] specifications, was used in the making of mortar samples.

2.1.2 Fine Aggregates:

Fine aggregates used for the preparation of cement mortar were obtained from the Sechelt pit in B.C. and had a relative dry density and absorption ratio of 2.651 and 0.79% respectively. The maximum size of fine aggregates was 4.75 mm.

2.1.3. Bacteria:

Bacillus subtilis is a gram-positive bacterium, also known as the *hay bacillus* or *grass bacillus*, found in the soil and the gastrointestinal tract of human and ruminants [28]. The Bacillus subtilis strain 168, cultured and grown at the microbiology laboratory of the University of Victoria, was used in this study.

The medium composition used for the growth of bacterial culture was Peptone 5 g/ Litre, NaCl 5 g/ Litre and Yeast Extract 3 g/ Litre. The medium was first sterilized by autoclaving at 121°C for 20 minutes. Then, the culture was incubated at 35°C with shaking at 200 rpm for 72 hours.

Microbial enumeration method was used to calculate the number of bacteria per ml of the solution. The serial dilutions plating and counting of live bacteria were done to determine the number of bacteria per ml of the solution. The 10 µL of four bacteria dilution samples (10^{-3},10^{-5}, 10^{-7}, 10^{-9}) were incubated on tryptone soya agar plates (see Figure 3) and the number of colony forming units (CFUs) was counted.

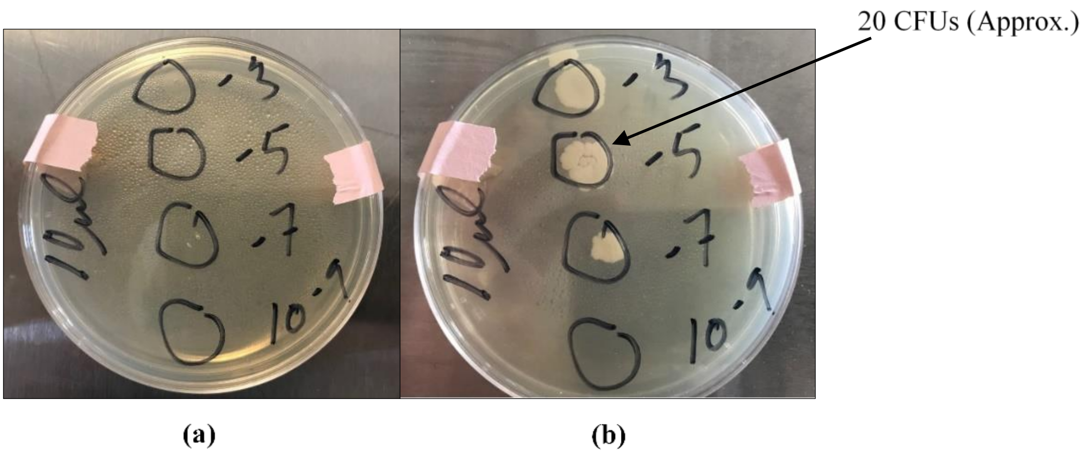

Figure 3: Bacteria colony forming units; (**a**) Plating of bacteria dilutions, (**b**) CFUs counting.

Dilution 10^{-5} had the most consistent number of CFUs for different plates. So, 10^{-5} dilution was used to calculate the number of bacteria/ml.

$$\frac{\text{Number of Colony Forming Units}}{\text{Volume plated (mL) x total dilution used}} \rightarrow \frac{20}{0.01\text{mL x } 10^{-5}} \rightarrow 2\text{x}10^{8} \text{ Bacteria/ml}$$

Hence the bacteria concentration was 2 x 10^8 bacteria per ml of the bacterial suspension.

2.1.4. Cellulose Fiber:

Fibers used in this study were obtained from Solomon colors, INC. These fibers are a special type of natural cellulose fibers called UltraFiber 500 made from Slash pines and Loblolly in North America. As per the manufacturer's declaration, UltraFiber 500 is an alkali-resistant cellulose based microfibers used for secondary reinforcement, provide crack control and have better hydration and bonding properties [29]. A close-up view of cellulose fibers is shown in Figure 4.

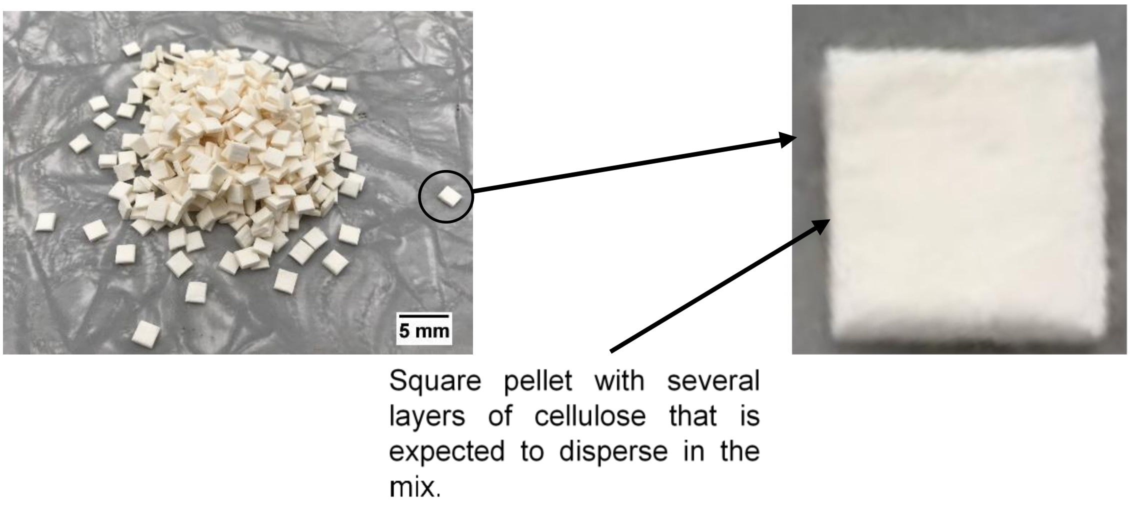

Figure 4: Micro cellulose fibers

Use of these fibers in cement mortar also supports the purpose of sustainability as they come from natural renewable resources. Apart from this, high surface area and close spacing of cellulose fibers make them quite effective in the suppression and stabilization of microcracks in the concrete matrix [30]. General properties of cellulose fibers are represented in Table 2.

Table 2: General Properties of UltraFiber 500 [31]

Name of Fiber	UltraFiber 500
Material Type	High Alkali Resistant, natural cellulose fibers
Average Length	2.1 mm
Average Denier	2.5 g/9,000m
Average Diameter	0.00063 inch
Count, fiber/lb	720,000,000
Density	1.10 g/cm^3
Surface Area	25,000 cm^2/g
Tensile Strength	750 N/mm^2
Average Elastic Modulus	8500 N/mm^2
Water Absorption	Up to 85% of fiber weight [22]

2.1.5. Calcium Lactate:

The calcium lactate is used as a nutrient for bacteria because it does not interfere with the setting time of the concrete. It is a white crystalline salt with chemical formula $C_6H_{10}CaO_6$. Calcium lactate for this study was purchased from iChemical Technology USA Inc. Table 3 shows the general properties of calcium lactate.

Table 3: General properties of calcium lactate [32]

Physical State	Powder
Colour	White
Boiling Point	227.6 ºC at 760 mmHg
Flash Point	109.9 ºC
Molecular Formula	$C_6H_{10}CaO_6$
Molecular Weight	218.22

2.2. Mortar Mix Design:

The cement/sand and water/cement ratios for mortar mix design were selected as 0.33 and 0.5 respectively, which represents a typical mix used in the field with a target strength of 32 Mpa. Singh and Gupta [33], used the 0.25% volume fraction of fibers to immobilize bacteria in their study and no visible healing of cracks was observed by them for this volume fraction of fibers. In this study, 0.5% volume fraction of cellulose fibers was used to increase the fibers available for bacteria absorption. Moreover, Banthia et al. also used the same volume fraction of cellulose fibers in their study on fiber reinforced concrete [34]. Four types of mixes were formulated:

1. **CMxx:** Control mortar.
2. **CO.5Mxx:** Control mortar with cellulose fibers equal to 0.5% of the volume fraction.
3. **BL0.5Mxx:** Mortar with *bacillus subtilis* equal to 1.3 x 10^7 bacteria/cm^3 of cement mortar absorbed in cellulose fibers (0.5% of the volume of mortar) and calcium lactate equal to 4.5% of cement weight.
4. **B0.5Mxx:** Mortar with *bacillus subtilis* equal to 1.3 x 10^7 bacteria/cm^3 of cement mortar absorbed in cellulose fibers (0.5% of the volume of mortar) and cured in water containing calcium lactate.

Where C, M, B, L, and xx refers to control, mortar, bacteria, calcium lactate, and sample number respectively. The decimal fraction indicates the percentage volume of cellulose fibers in cement mortar. Mix proportions used for mortar are represented in Table 4.

Table 4: Mix proportions for cement mortar

Material	**Quantities**	**Units and Remarks**
Cement	736	
Sand	2207	
Water	368	Kg/m^3
Cellulose Fibers 0% and 0.5%	0 and 5.5	
Bacterial Solution (2x10^8 bacteria/ml)	0.065	ml/cm^3 to achieve 1.3 x 10^7 bacteria/cm^3 of cement mortar
Calcium Lactate (4.5% of cement weight)	33.12	Kg/m^3

2.3. Absorption of Bacteria in Cellulose Fiber:

The required quantity of cellulose fibers was kept soaked in the required quantity of bacterial solution for BL0.5Mxx and B0.5Mxx mixes for 24 hours (see Figure 5). The 85% absorption capacity of fibers by weight results in 9.3 x 10^5 immobilized bacteria/cm^3 of mortar.

Figure 5: Bacteria absorbed in cellulose fibers.

2.4. Mixing Curing and Setting Procedure:

Ingredients for different mixes were batched out as per the final volume of mortar required by using an electronic weighing balance. A homogeneous mixture of cellulose fibers was achieved by preparing a fiber mixture in bacterial solution, followed by mixing in the sand for a minute using a table mixer. Afterward, required cement and water quantities were added to the paste, calcium lactate was added for BL0.5Mxx mix and mixed for another minute. The amount of water used for each mix was adjusted for the amount of bacterial solution used. Once the uniform mix was achieved, the mortar was placed into cube molds of size 50 mm, shown in Figure 6.

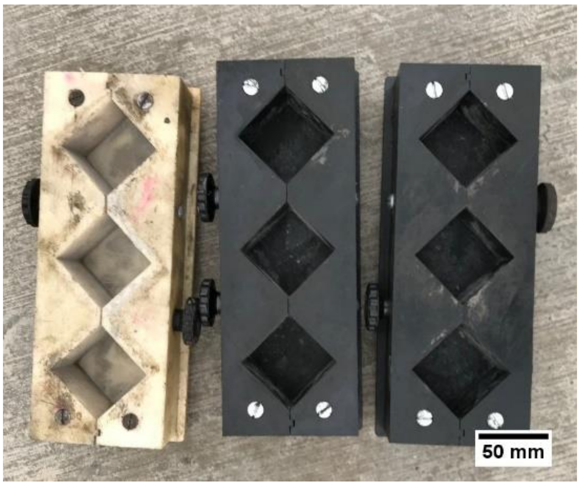

Figure 6: Cube molds

To ensure maximum compaction and removal of entrapped air, manual compaction was done using a tamping rod. The mortar was placed in molds in two equal layers and each layer was tamped 25 times. After compaction, molds were covered with a plastic sheet and placed at room temperature for the next 24 hours. Demolding was carried out after 24 hours and samples were placed in a water tub maintained at 23 ± 2° C after appropriate labeling based on the mix design. The bacterial mix without calcium lactate (B0.5Mxx) was cured in water containing calcium lactate. The amount of calcium lactate added to curing water was equal to 4.5% of the cement content of the cubes cured in that water.

Figure 7 shows the preparation of self-healing mortar by using cellulose fiber as a bacteria-carrier. The cellulose fibers were kept soaked in bacterial suspension for 24 hours to absorb bacteria. Bacterial nutrient, calcium lactate was mixed with mortar ingredients for BL0.5Mxx mix and mixed in curing water for B0.5Mxx specimens. As far as dispersion of these fibers is concerned, it is reported [34] that these cellulose fibers are hydrophilic in nature and each chip disperses into 30,000 individual fibers. To investigate the dispersion of fibers and homogeneity of the mortar matrix, visual observations were made in this study both during the fresh mixing stage and on cracked specimens. Use of microscopy (like SEM) was beyond the scope of the current work.

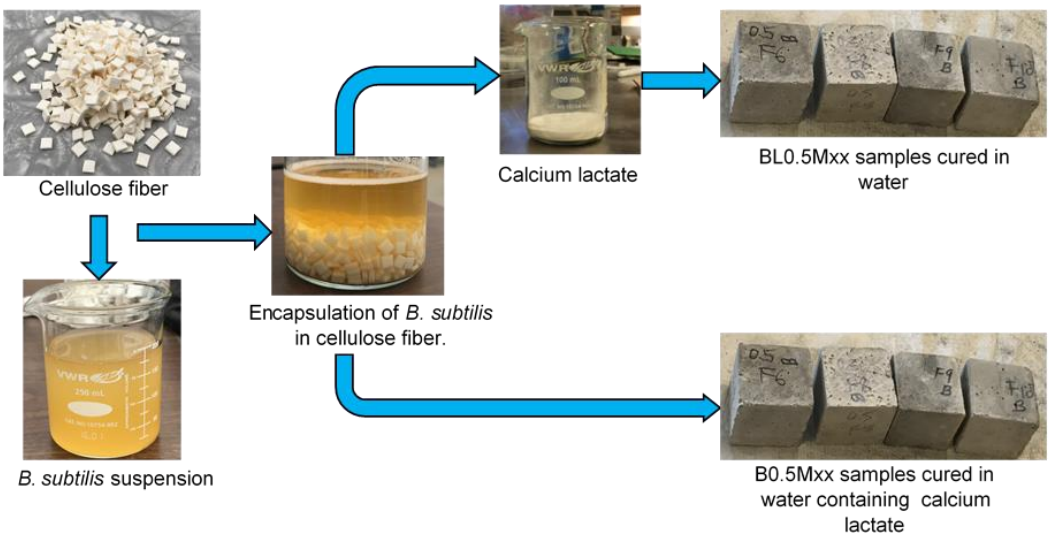

Figure 7: Preparation of self-healing mortar specimens using cellulose fiber as a carrier for bacteria

2.5. Test Specimens:

Fifteen mortar cubes of size 50 mm were prepared for each mix (CMxx, C0.5Mxx, BL0.5Mxx and B0.5Mxx), resulting in a total of 60 specimens. Table 5 summarizes the specimens' type and quantity as well as curing age used in different test methods.

Table 5. Type, number and curing age of specimens used in different test methods

Test method	Number of specimens	Type of specimen	Curing Age
UPV and Image Analysis	5	Cube (50 mm)	14 days
UPV and Image Analysis	5	Cube (50 mm)	28 days
Compressive Strength	5	Cube (50 mm)	28 days

The cubes of size 50 mm were chosen as the only limited amount of bacteria could be cultured in the laboratory.

2.6. Testing Procedure:

Three types of tests were conducted to investigate the self-healing and strength performance of all mixes. The self-healing tests were performed to evaluate the self-healing efficiency and a compression test was used to determine the strength properties of the mortar mixes.

2.6.1. Self-Healing Evaluation:

Two tests were performed to evaluate the self-healing efficiency of mortar mixes which are explained below.

2.6.1.1. Visual Inspection of Cracks:

The specimens prepared to monitor self-healing were pre-cracked after 14 and 28 days of curing. Cracks were induced in the cubes by using a standard crack inducing jig (SCIJ) [35], shown in Figure 8.

This jig uses the V-shaped cutting edges that act as stress concentrators. The cube was assembled inside the jig and the compression machine was used to subject compressive loading till visible cracks appeared on the surface of the cube. After inducing a crack, images of the cubes were taken and analyzed using a software *ImageJ* to determine the average width of the crack. The pre-cracked specimens were continued to cure in water to self-heal. After pre-cracking, images were taken after regular intervals of 7, 14 and 21 days. Pre-cracked images were compared with later days to see the evidence of any healing of cracks on the surface due to bacterial activity.

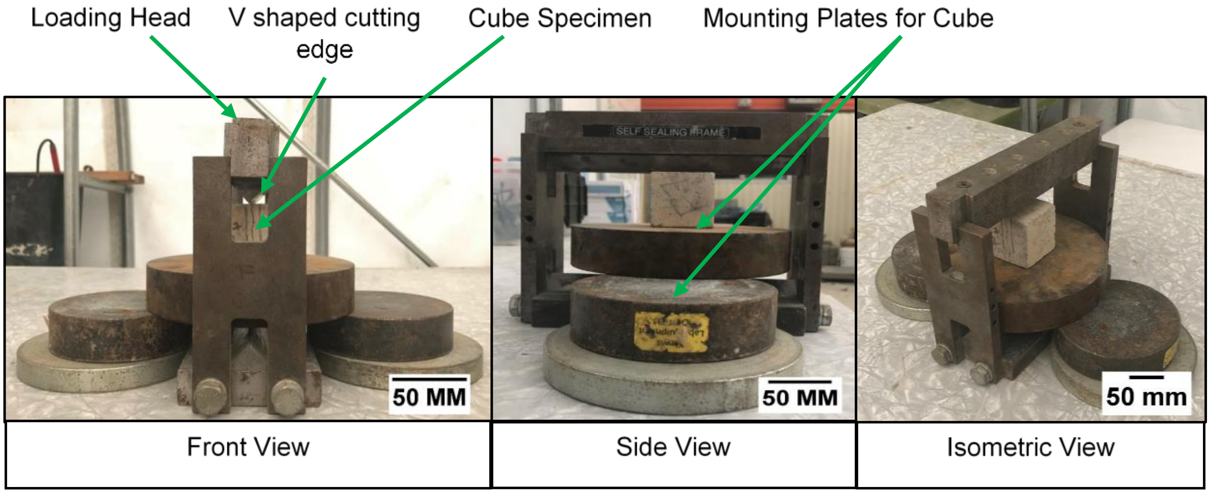

Figure 8: Crack Inducing Mechanism

2.6.1.2. Ultrasonic Pulse Velocity (UPV) Test:

UPV test is a very sensitive indicator of the presence of damage (cracks/flaws) in concrete, performed under laboratory conditions [36]. Ariffin et al. [37], Bahrin et al. [38] and Sarkar et al. [39] also used the UPV test to evaluate the self-healing performance of mortar. UPV test was performed on samples as per C597-16 [40]. The longitudinal stress wave was propagated through the mortar samples and time required to travel the wave across the sample was recorded. The travel time of the wave varies as a function of the density of the material, allowing the estimation of the discontinuities in the samples. Figure 9 and Figure 10 shows the sequence and arrangement for the UPV test respectively.

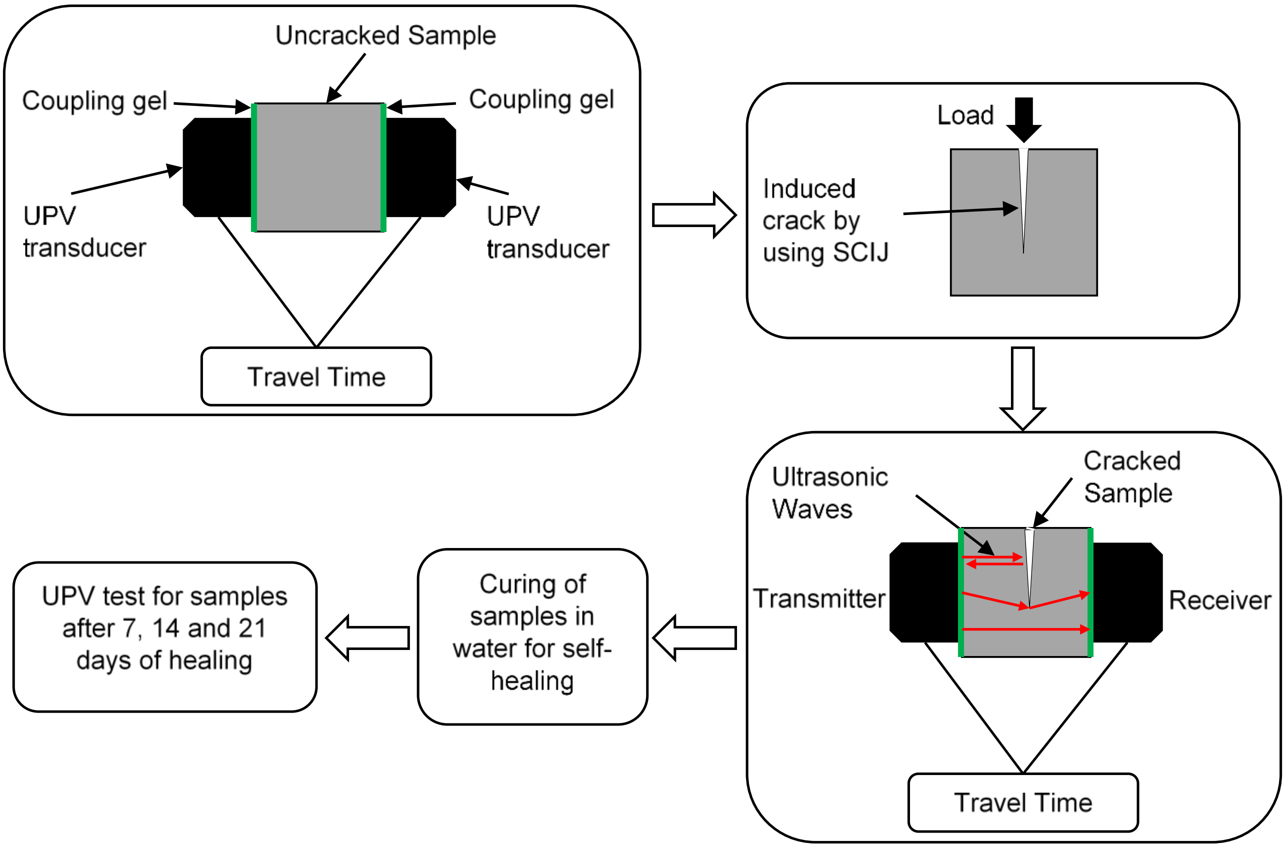

Figure 9: Sequence of UPV test to evaluate self-healing efficiency of mortar mixes

Figure 10: UPV Test Arrangement

The device consists of two transducers one to transmit the ultrasonic wave and the other to receive it. Both transducers were connected with the surface of the mortar samples and time required to travel the sound wave across the sample was recorded with a precision of at least 0.1 µs. The coupling gel was applied on the surface to get a better contact area, required for accurate results. The test was performed at a frequency of 150 kHz. The velocity of the ultrasonic wave was calculated using the formula below:

$V = D/T$, D = dimension of sample, 50 mm, T = Time required to travel the distance, D.

The test was performed on the uncracked and pre-cracked samples at the age of 14 and 28 days, followed by 7, 14 and 21 days of healing. The 14 and 28 days pre-cracked samples were used to observe the impact of age of the mortar on self-healing performance.

2.6.1.3. Compression Test:

Cubes were tested after 28 days of curing to determine the strength of mortar. Five cubes were tested for each type of mix to determine the average compressive strength. ASTM C579 [41] states the method to determine the compressive strength of cement mortar cubes of size 50mm. Uniaxial compression testing machine was used to test the cubes and the peak load was recorded at the point of failure. The loading rate was used within the range specified by the standard.

3. Results and Discussion:

3.1. Self-Healing Based on Image Analysis

Table 6 shows the crack widths for samples pre-cracked at the age of 14 and 28 days of curing for all mixes.

Table 6. Average crack width of pre-cracked samples

Mix Design	**14 days cured**		**28 days cured**	
	Sample Name	**Average Crack Width (mm)**	**Sample Name**	**Average Crack Width (mm)**
CMxx	CM1	0.46	CM6	0.58
	CM2	0.62	CM7	0.61
	CM3	0.54	CM8	0.50
	CM4	0.5	-	-
C0.5Mxx	C0.5M1	0.27	C0.5M6	0.29
	C0.5M2	0.80	C0.5M7	0.27
	C0.5M3	0.31	C0.5M8	0.38
	C0.5M4	0.29	C0.5M9	0.38
	C0.5M5	0.30	C0.5M10	0.37
BL0.5Mxx	BL0.5M1	0.49	BL0.5M6	0.59
	BL0.5M2	0.68	BL0.5M7	0.70
	BL0.5M3	0.69	BL0.5M8	0.67
	BL0.5M4	0.45	BL0.5M9	0.58
B0.5Mxx	B0.5M1	0.56	B0.5M6	0.50
	B0.5M2	0.57	B0.5M7	0.68
	B0.5M3	0.74	B0.5M8	0.63
	B0.5M4	0.60	-	-

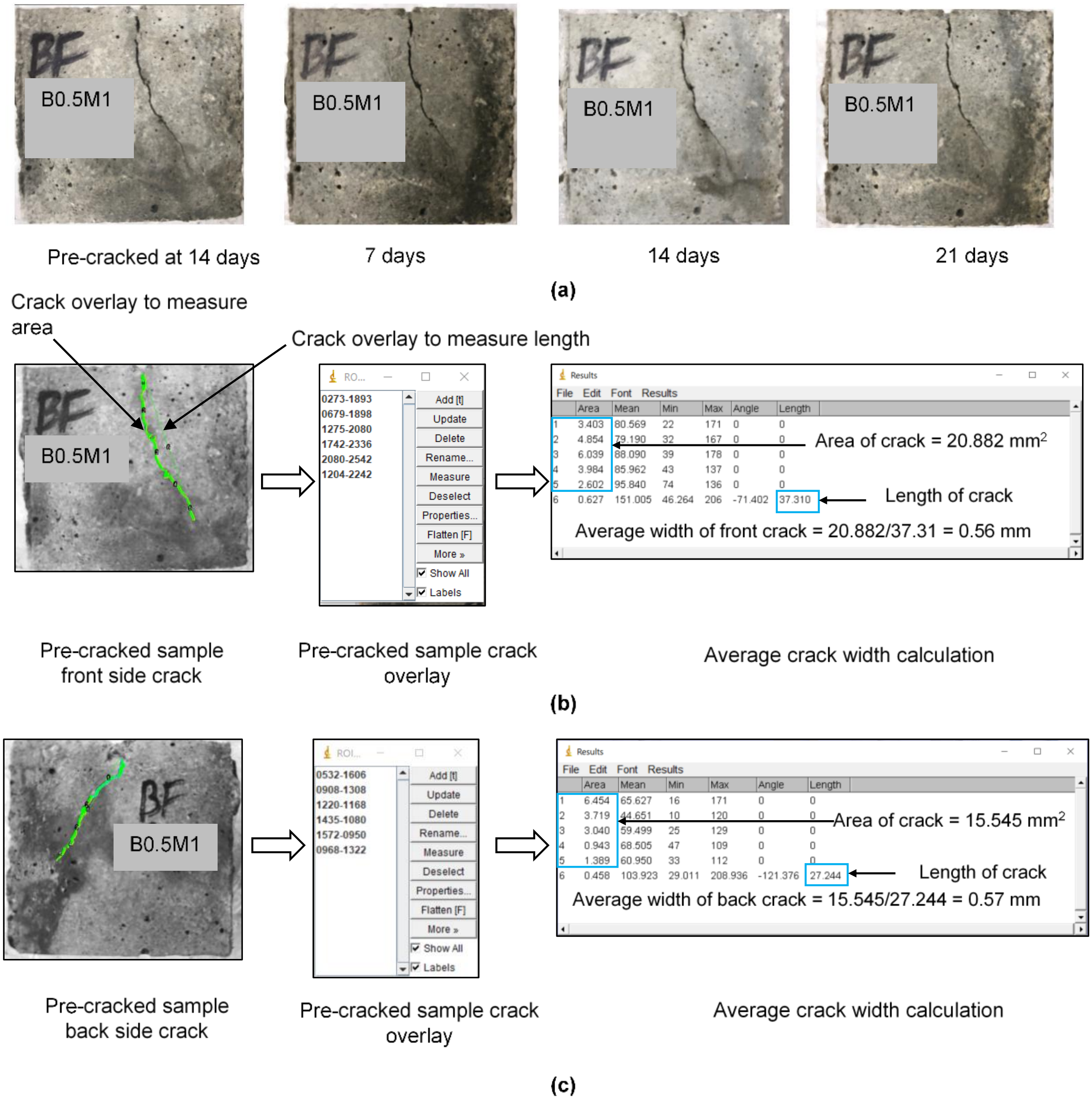

Figure 11. Image analysis for B0.5M1; (**a**) Image comparison on the front side of the cube; (**b**) Front side crack; (**c**) Backside crack.

Crack width = (crack width on front side + crack width on backside)/2 = (0.56+0.57)/2 =0.56 mm.

Images were analyzed to determine the average crack width of the samples for different stages of self-healing by using *imageJ* software. First, area and length of crack were determined. The average width of the crack was determined using the following formula:

Width of Crack = Area of Crack/Length of Crack

No visible healing of the cracks was observed on the surface of the cracks in image analysis for all types of mixes. Figure 11 (a) shows the sample of images for B0.5M1 mortar pre-cracked at 14 days of curing and observed for crack healing after 7, 14 and 21 days on the front side of the cube. Figure 11 (b) and Figure 11 (c) show the image analysis to measure the crack width of pre-cracked sample on the front and backside of the sample respectively. The average crack width for the sample was calculated from the average of front and backside crack widths.

3.2. Self-Healing Based on UPV Test

The self-healing performance of all mortar mixes was investigated by the UPV test. The UPV technique used to evaluate self-healing is the same as used by Ariffin et al. [37], Bahrin et al. [38] and Sarkar et al. [39]. The UPV time was recorded for all the mortar samples at different stages of healing across the crack to study any interior healing of the cracks. For each sample test was repeated at least three times. Data are presented as average ± standard deviation. Table 7 and Table 8 show the UPV results for all mortars cured for 14 and 28 days respectively.

Same as done by Zhong and Yao [42], the microstructure changes in mortar are inferred from the decrease of UPV by introducing a damaged degree defined as:

$$D = 1 - \frac{V_p}{V_0} \quad (1)$$

Where D is the damaged degree of the mortar, V_p is UPV of the pre-cracked sample, and V_0 is the UPV of an uncracked sample.

A percentage self-healing of mortar, *SH*, that incorporates UPV after 21 days of self-healing and pre-cracked sample can be introduced as:

$$SH = \frac{(V_{21} - V_p)}{V_p} \times 100 \quad (2)$$

Where V_{21} is the UPV after 21 days of self-healing, and V_p is the UPV of pre-cracked sample.

Table 7. UPV results for samples pre-cracked at 14 days

Mix design	Sample name	UPV (km/s) ± STDV					Damaged degree	% Self-healing ± STDV
		14 days uncracked (V_0)	14 days pre - cracked (V_p)	7 days healed	14 days healed	21 days healed (V_{21})	$D = 1-(V_p/V_0)$	$SH = (V_{21}-V_p)$ x100/V_p
CMxx	CM1	4.59 ± 0	3.97 ± 0.07	4.39 ± 0	4.39 ± 0	4.39 ± 0	0.13	10.5 ± 1.9
	CM2	4.46 ± 0.06	4.08 ± 0.06	4.39 ± 0	4.39 ± 0	4.39 ± 0	0.09	7.6 ± 1.7
	CM3	4.53 ± 0.04	4.16 ± 0.03	4.39 ± 0	4.39 ± 0	4.39 ± 0	0.08	5.6 ± 0.8
	CM4	4.53 ± 0.04	4.02 ± 0.02	4.2 ± 0	4.39 ± 0	4.39 ± 0	0.11	9.1 ± 0.4
C0.5Mxx	C0.5M1	4.26 ± 0.09	3.26 ± 0.02	3.46 ± 0.01	3.61 ± 0.01	3.73 ± 0	0.24	14.4 ± 0.7
	C0.5M2	4.4 ± 0.02	3.9 ± 0.01	4 ± 0	4.13 ± 0	4.2 ± 0	0.11	7.8 ± 0.4
	C0.5M3	4.39 ± 0	3.98 ± 0.03	4.11 ± 0.02	4.17 ± 0	4.24 ± 0	0.09	6.5 ± 0.8
	C0.5M4	4.39 ± 0	3.92 ± 0.01	4.09 ± 0.02	4.13 ± 0	4.17 ± 0	0.11	6.4 ± 0.4
	C0.5M5	4.37 ± 0.02	3.82 ± 0	4 ± 0	4.1 ± 0	4.17 ± 0	0.13	9.2 ± 0
BL0.5Mxx	BL0.5M1	4.39 ± 0	3.55 ± 0.02	3.88 ± 0	3.93 ± 0.07	4.03 ± 0	0.19	13.4 ± 0.8
	BL0.5M2	4.2 ± 0	2.12 ± 0.01	4.03 ± 0	4.2 ± 0	4.2 ± 0	0.50	98.3 ± 1.4
	BL0.5M3	4.37 ± 0.05	2.71 ± 0.01	3.73 ± 0	3.98 ± 0.07	4.2 ± 0	0.38	54.9 ± 0.4
	BL0.5M4	4.37 ± 0.08	3.8 ± 0.01	3.88 ± 0	4.2 ± 0	4.2 ± 0	0.13	10.6 ± 0.4
B0.5Mxx	B0.5M1	4.6 ± 0.02	2.3 ± 0.01	3.66 ± 0.06	3.73 ± 0	3.9 ± 0.03	0.50	69.1 ± 1.8
	B0.5M2	4.4 ± 0.02	3.88 ± 0.02	4.2 ± 0	4.2 ± 0	4.24 ± 0	0.12	9.3 ± 0.7
	B0.5M3	4.6 ± 0.02	2.16 ± 0	3.98 ± 0.07	4.1 ± 0	4.2 ± 0	0.53	94.7 ± 0.4
	B0.5M4	4.39 ± 0	2.76 ± 0.01	4.01 ± 0.03	4.05 ± 0.03	4.2 ± 0	0.37	52.1 ± 0.7

Table 8. UPV results for samples pre-cracked at 28 days

Mix design	Sample name	UPV (km/s) ± STDV					Damaged degree	% self-healing ± STDV
		28 days uncracked (V_0)	28 days pre - cracked (V_p)	7 days healed	14 days healed	21 days healed (V_{21})	D = 1-(V_p/V_0)	SH = (V_{21}-V_p) x100/V_p
CMxx	CM6	4.59 ± 0	3.95 ± 0.06	4.2 ± 0	4.2 ± 0	4.2 ± 0	0.14	6.3 ± 1.6
	CM7	4.59 ± 0	4.03 ± 0	4.39 ± 0	4.39 ± 0	4.39 ± 0	0.12	8.8 ± 0
	CM8	4.6 ± 0.04	4.14 ± 0.07	4.39 ± 0	4.39 ± 0	4.39 ± 0	0.10	5.8 ± 1.7
C0.5Mxx	C0.5M6	4.39 ± 0	3.92 ± 0.01	4.23 ± 0.02	4.24 ± 0	4.24 ± 0	0.11	8.2 ± 0.4
	C0.5M7	4.55 ± 0.12	3.9 ± 0.01	4.2 ± 0	4.21 ± 0.02	4.23 ± 0.02	0.14	8.5 ± 0.7
	C0.5M8	4.53 ± 0.11	3.55 ± 0.05	3.94 ± 0	3.96 ± 0.01	3.99 ± 0.03	0.22	12.5 ± 1.3
	C0.5M9	4.39 ± 0	3.73 ± 0.04	4.04 ± 0.02	4.09 ± 0.02	4.11 ± 0.02	0.15	10.1 ± 1.4
	C0.5M10	4.39 ± 0	3.98 ± 0.06	4.2 ± 0	4.2 ± 0	4.23 ± 0.02	0.09	6.2 ± 1.4
BL0.5Mxx	BL0.5M6	4.39 ± 0	3.51 ± 0.03	4.2 ± 0	4.2 ± 0	4.36 ± 0.04	0.20	24.1 ± 2
	BL0.5M7	4.36 ± 0.04	3.86 ± 0.03	4.2 ± 0	4.2 ± 0	4.2 ± 0	0.12	9 ± 0.8
	BL0.5M8	4.32 ± 0.05	3.87 ± 0.01	4.03 ± 0	4.2 ± 0	4.2 ± 0	0.11	8.7 ± 0.4
	BL0.5M9	4.32 ± 0.05	3.59 ± 0.01	4.03 ± 0	4.03 ± 0	4.03 ± 0	0.17	12.4 ± 0.4
B0.5Mxx	B0.5M6	4.43 ± 0.06	4.05 ± 0.03	4.2 ± 0	4.2 ± 0	4.2 ± 0	0.08	3.6 ± 0.8
	B0.5M7	4.45 ± 0.05	3.73 ± 0	4.39 ± 0	4.39 ± 0	4.39 ± 0	0.16	17.5 ± 0
	B0.5M8	4.59 ± 0	3.89 ± 0.01	4.39 ± 0	4.39 ± 0	4.39 ± 0	0.15	12.9 ± 0.4

Mixes were compared based on the damaged degree instead of crack widths because induced cracks have varying widths and depths. Based on the availability and distribution of results, the data were averaged for damaged degree between 0.1 and 0.2 for all mixes. Figure 12 and Figure 13 show the curing days-UPV relation and *SH* for 14 and 28 days aged pre-cracked samples, respectively for *D* between 0.1 and 0.2 for all mixes.

Zhong and Yao [42] explained in their study, the UPV of concrete is a combined effect of the matrix, microcracks, and macrocracks, which could be represented as:

$$V_c = \frac{1}{\frac{i_1}{V_1}+\frac{i_2}{V_2}+\frac{i_3}{V_3}} \quad (3)$$

Where V_c is the UPV of concrete, i_1, i_2, i_3 and V_1, V_2, V_3 are the volume fraction and UPV of the matrix, microcracks, and macrocracks respectively. V_1 is a function of elastic modulus, Poisson's ratio, inner friction angle and material fraction toughness of the matrix. V_2 can be expressed as a function of microcracks parameters such as half-length, shape ratio and density of microcracks. Whereas, V_3 for macrocracks is ultrasonic wave velocity in the air (340 m/s). Increase of elastic modulus and material fracture toughness results in an increase of V_1, while the increase of half-length, shape ratio and density of microcracks lead to the decrease of V_2.

UPV is mostly influenced by V_1 for uncracked samples and it is close to intact mortar matrix due to less volume of microcracks in the uncracked sample. Once the mortar is cracked, the uncracked matrix volume i_1 decreases greatly, while i_2 and i_3 increase compatibly. Cracking of mortar results in the increase of microcracks density leads to a decrease of V_2, thus UPV of cracked mortar decreases greatly. Once the cracked samples are cured in water for self-healing, re-hydration products or calcium carbonate from MICP crystallized inside the cracks, results in a decrease of i_2 and i_3. The crystallization also changes the inner microcracks and porous structure, results in an increase of V_2, thus UPV of self-healed mortar increases.

From Figure 12 and Figure 13, it appears that the presence of fibers decreases the UPV slightly for uncracked samples. This is expected as UPV through cellulose is lower than mortar. This trend is observed both at 14 and 28 days. Cracking decreases the UPV for all mixes which indicates the discontinuity due to cracking. It can be observed, curing time results in an increase in UPV for all mixes, indicates the self-healing process working well inside the cracks.

From Figure 12, it can be observed, controlled and only fiber mortar samples showed a *SH* of 9.8% and 7.8% respectively. This can be attributed due to continued hydration process of unhydrated cement particles at an early age. C0.5Mxx have less *SH* compare to control mix, indicates fiber addition results in a decrease in *SH*, this is due to less availability of unhydrated cement particles as compared to control mix, because 0.5% volume fraction of matrix replaced with fibers. The self-healing is bacterial mixes was attributed due to precipitation of calcium carbonate as per reaction (equation 4) due to bacterial activities [1]. 9.32% self-healing is observed in the B0.5Mxx, more than mortar containing only fibers. Mix BL0.5Mxx incorporated with cellulose fiber as a carrier for bacteria, and nutrients are provided inside the mix shows 12.04% *SH*, maximum as compared to other mixes. This is due to the availability of calcium lactate throughout the matrix for the MICP results in more availability of carbon dioxide inside the matrix, which results in the additional production of calcium carbonate as per reaction (equation 5) [1], due to the carbonation of calcium hydroxide, one of the major hydration products of cement.

$$\mathrm{CaC_6H_{10}O_6} + 6\mathrm{O_2} \longrightarrow \mathrm{CaCO_3} + 5\mathrm{CO_2} + 5\mathrm{H_2O} \tag{4}$$

$$\mathrm{CO_2} + \mathrm{Ca(OH)_2} \longrightarrow \mathrm{CaCO_3} + \mathrm{H_2O} \tag{5}$$

However, in case of B0.5Mxx calcium lactate is only present in cracked region through curing water for MICP and carbonation of calcium hydroxide possible only in the cracked region instead of the whole matrix like BL0.5Mxx, results in slightly less *SH* as compared to BL0.5Mxx for samples cracked at an early age.

Figure 13 illustrates the self-healing for samples pre-cracked at 28 days of curing. It can be observed *SH* in control mortar is decreased to 6.97% for 28 days pre-cracked samples as compared to 9.8% for 14 days pre-cracked samples. This exhibit, there are less unhydrated cement grains to contribute for the self-healing at later age. Both bacterial mixes, BL0.5Mxx and B0.5Mxx show the higher *SH* than control and only fiber mix, 10%, and 15.2% respectively.

Like control mix, BL0.5Mxx results in a decrease in *SH* for samples pre-cracked at 28 days as compared to 14 days. Because at 28 days age there is less availability of calcium hydroxide to produce calcium carbonate inside the matrix and lower availability of calcium lactate in the cracked region for MICP, results a decrease in reactions (3) and (4). However, in the case of B0.5Mxx more calcium lactate from curing water is present in the cracked region for MICP results an increase in reaction (3) and leads to maximum self-healing performance among all mixes.

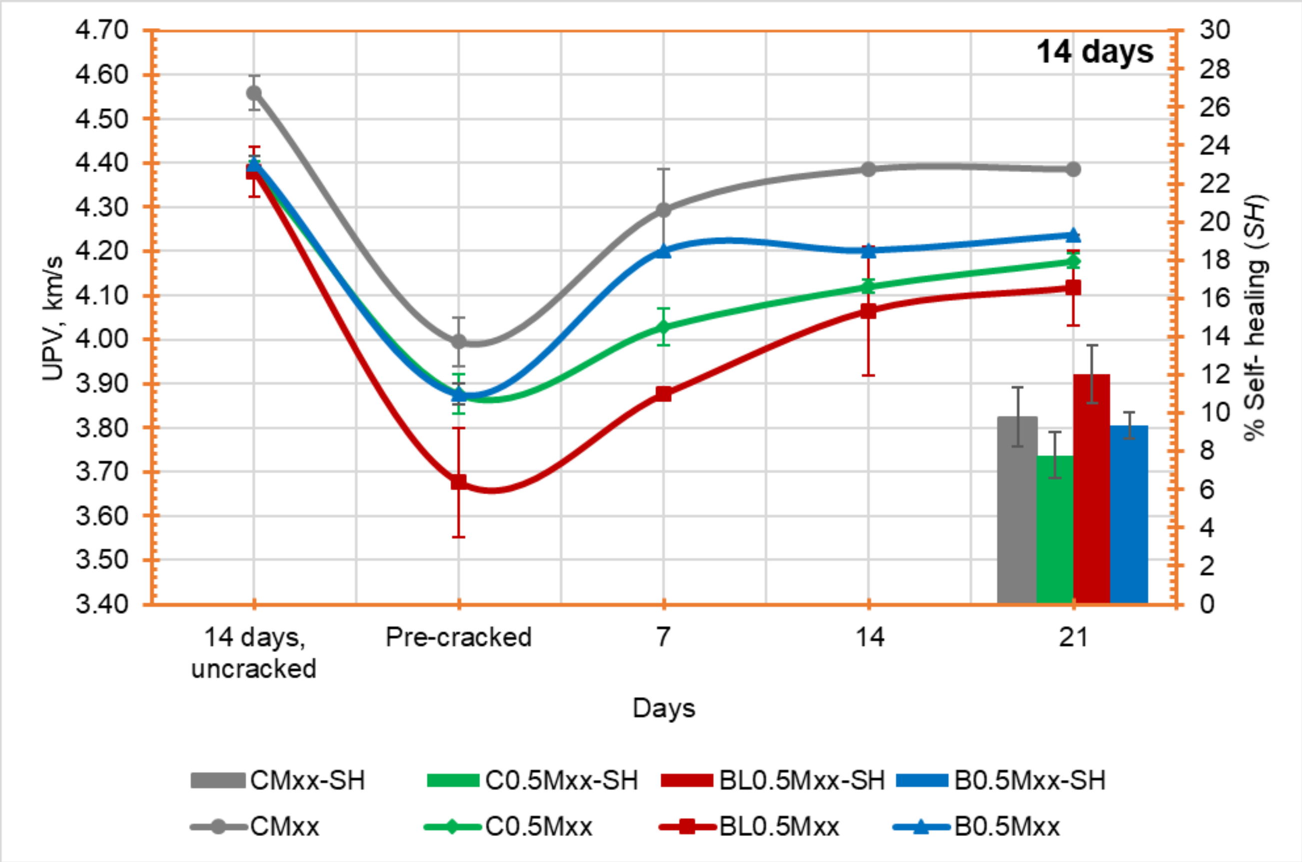

Figure 12. UPV at different days of curing and *SH* for all mixes (D = 0.1 to 0.2) pre-cracked at 14 days

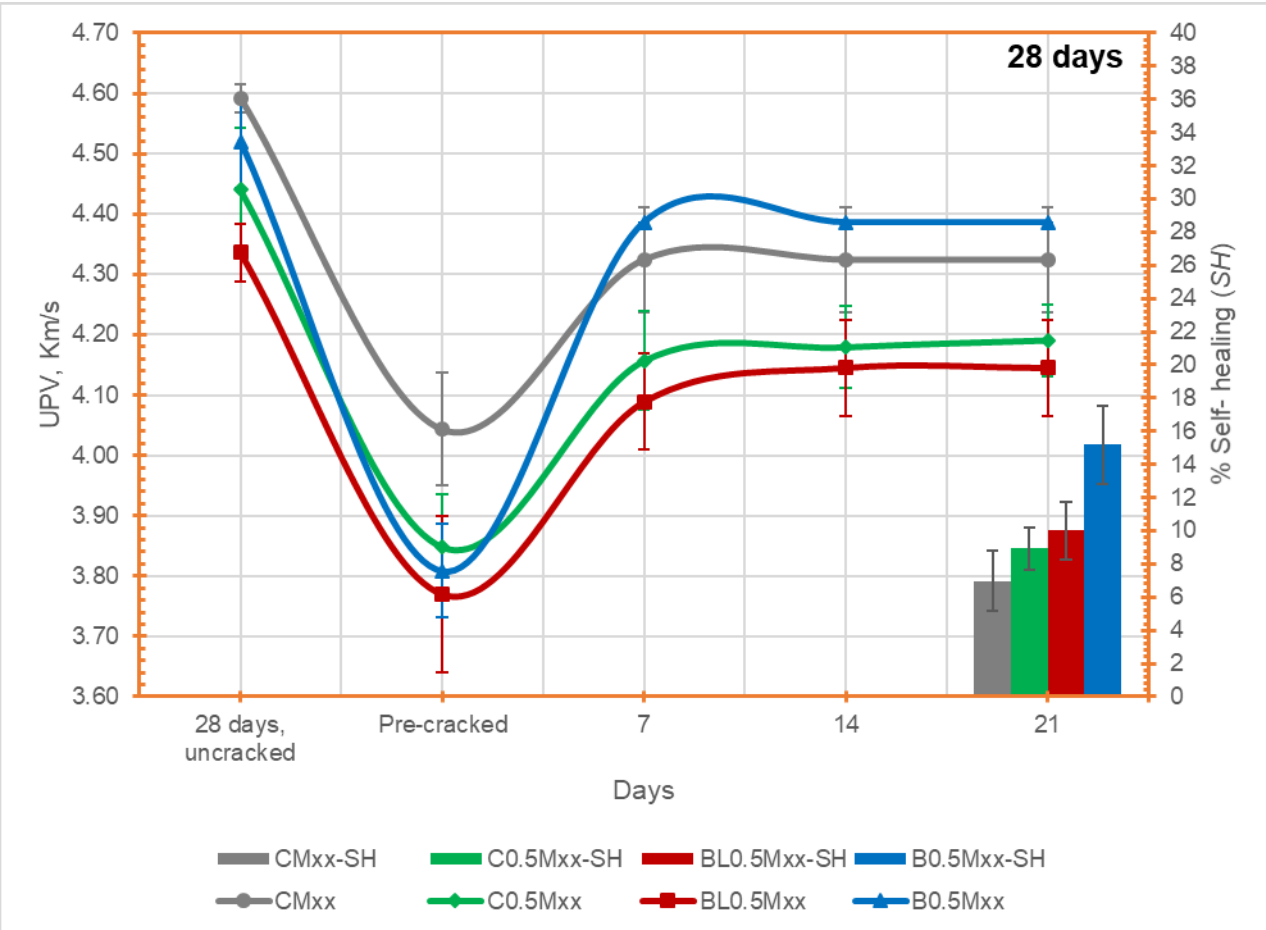

Figure 13. UPV at different days of curing and *SH* for all mixes (D = 0.1 to 0.2) pre-cracked at 28 days

Figure 14 and Figure 15 represents the relation between damaged degree and percentage self-healing for samples pre-cracked at the age of 14 and 28 days respectively. It appears that *SH* is virtually dependent on the damaged degree when the results are presented as trendlines. It can be observed that *SH* is increased as *D* increases for all mixes pre-cracked at 14 and 28 days. Bacterial mixes show significantly improve in *SH* at higher damaged degree, BL0.5Mxx results in 13.2% and 64.1% more *SH* than control mix at *D* of 0.2 and 0.5 respectively, for 14 days pre-cracked samples (see Figure 14). Similarly, 3.18% and 11.62% more *SH* is observed in B0.5Mxx at D of 0.12 and 0.2 respectively, for samples pre-cracked at 28 days (see Figure 15). This is because, higher *D* results in more availability of water and oxygen through microcracks, which improves the MICP, leads to a higher value of *SH* at increased *D*. However, Zhong and Yao defined a damaged threshold beyond that self-healing decreases as D increases, for normal concrete damage threshold is about 0.6-0.7 [42].

Relating, Figure 14 and Figure 15, demonstrate a decrease in *SH* performance of bacterial mixes with age of pre-cracking, 13.2% to 5.3% decrease in *SH* for BL0.5Mxx for D of 0.2. This decrease in *SH* of bacterial mixes can be due to continued hydration reaction in mortar resulting in the development of dense microstructure at later age. The dense matrix creates pressure on the fibers and free bacteria, leads to a decrease in the viability of bacteria and therefore, the self-healing process decreased at later age. Additionally, at a later age, less availability of calcium hydroxide from cement hydration reaction leads to lower precipitation of calcium carbonate from the carbonation of calcium hydroxide.

Even after a decrease in *SH* with age, both mixes with bacteria absorbed in fibers exhibit higher *SH* than control and only fiber mixes. Therefore, the technique using cellulose fiber as a bacteria-carrier was effective and improved the self-healing capacity of control mortar.

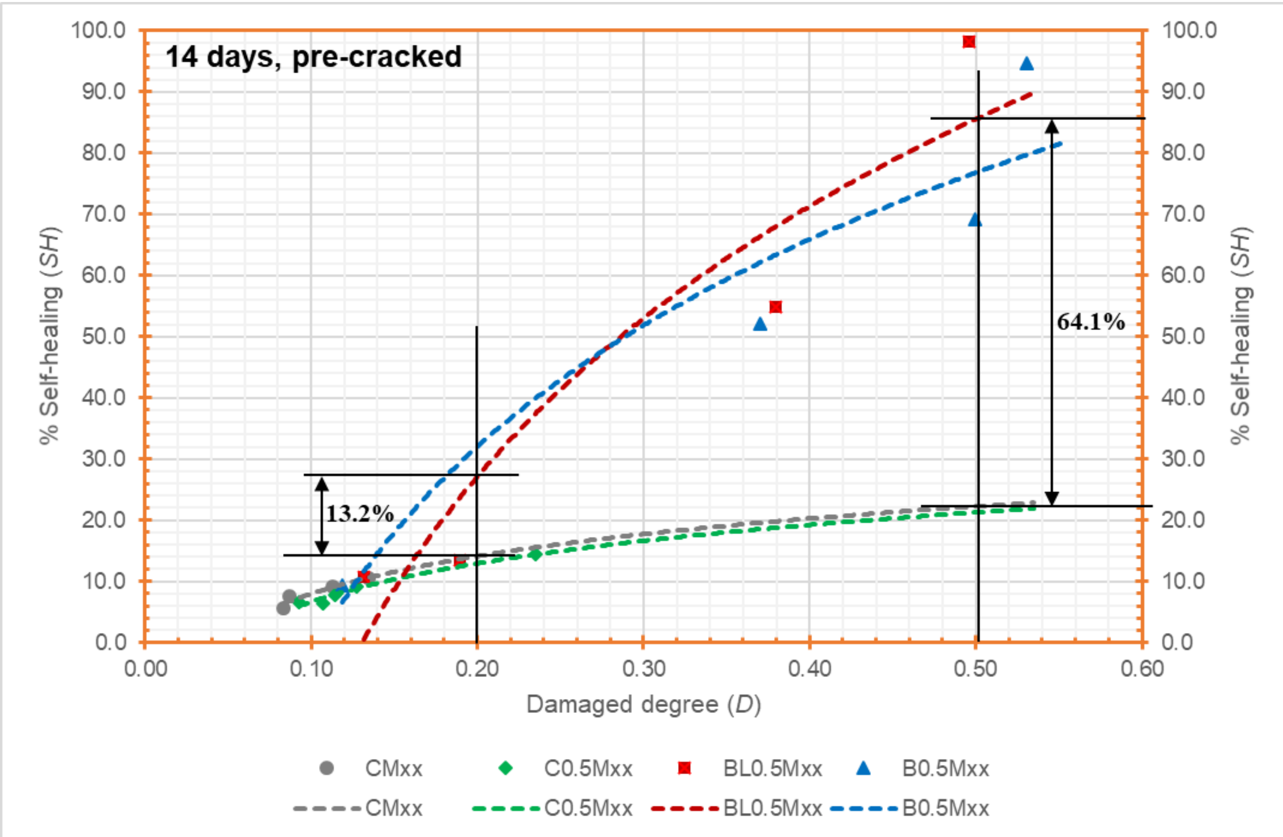

Figure 14. *D* and *SH* relations of samples pre-cracked at 14 days

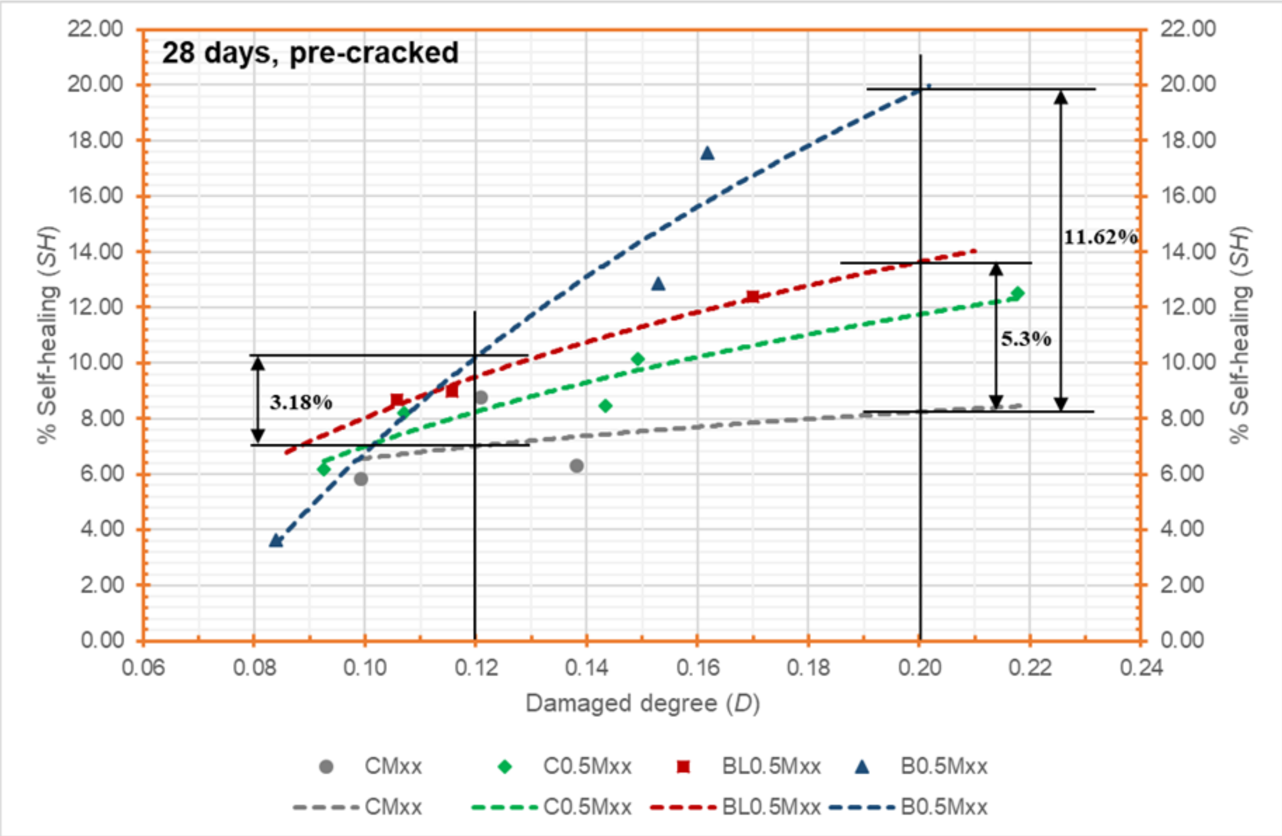

Figure 15. *D* and *SH* relations of samples pre-cracked at 28 days

3.3 Compressive Strength:

28 days compressive strength for all four mixes was measured as per ASTM C579 [41] after wet curing. Table 9 shows the average compressive strength of each mix along with averages and standard deviation values.

Table 9. Compressive strength test results for cement mortar

Mix Design	28 days Compressive Strength (MPa)	
	Individual	Average ± STDV
CMxx	48.12 40.4 49.54 46.82 48.04	46.58 ± 3.21
C0.5Mxx	42.8 44.82 41.8 43.32 43.94	43.34 ± 1.02
BL0.5Mxx	30.5 32.3 28.54 30.78 33.68	31.16 ± 1.74
B0.5Mxx	39.36 34.04 35.88 35.9	36.29 ± 1.92

The data in Table 9 were analyzed for the % change in compressive strength from control mortar for all mixes. The % change in compressive strength for 28 days cured mortar is shown in Figure 16.

A decrease in compressive strength of mortar by 6.97% is noticed with addition of 0.5% fibers. This decrease in compressive strength is possibly attributed to the loss of workability of mortar when 0.5% by volume cellulose fibers are added, which causes lower compaction of mortar samples. Out of two bacterial mortar mixes, the maximum decrease in compressive strength is for BL0.5Mxx mix, 33.11%. However, a decrease of 22.09% in compressive strength is observed for the B0.5Mxx mix. Overall, it can be observed that the addition of bacteria and fibers results in a decrease in compressive strength of mortar. The more decrease in compressive strength is noticed in the mix containing calcium lactate. This is due to calcium lactate added to mortar do not take part in hydration of cement directly, instead, the by-product, calcium carbonate produced inside the mortar matrix and excess production of calcium carbonate inside the matrix causes reduction of compressive strength [43]. Opposite to this, mortar sample containing fiber and bacteria, cured in calcium lactate (B0.5Mxx) results in a lower decrease in compressive strength. However, the loss in strength is only for the limited mixes with 0.5% of fiber concentration and 1.3 x 10^7 bacteria/cm^3 concentration of bacteria. The change in compressive strength with different concentration of fibers, nutrients, and bacteria needs further investigation.

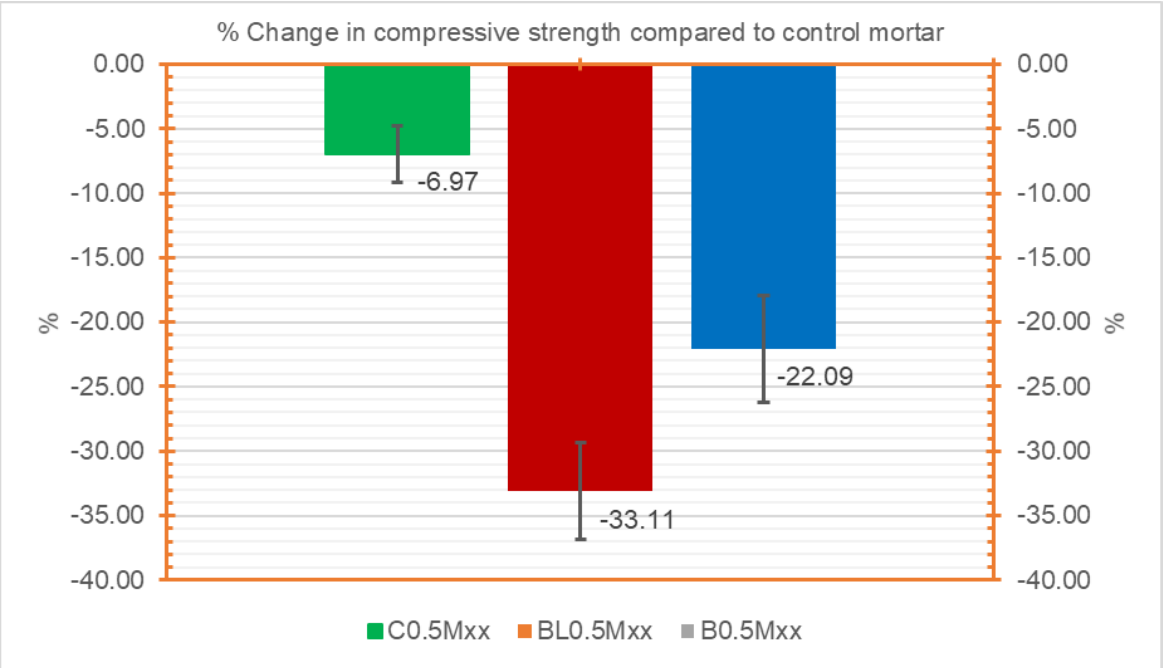

Figure 16. % Change in compressive strength compared to control mortar

The B0.5Mxx mix cured in water containing calcium lactate performed well to maintain the strength of mortar out of both bacterial mixes. So, it is observed that providing bacterial nutrients from outside during curing instead of inside while mixing helps to maintain the mortar strength properties.

3.4. Cost analysis of various bacteria-carriers:

The cost for different bacteria-carriers is figured out and compared for per cubic meter of concrete. The concrete mix design with a strength of 32 MPa is considered for the material calculation. The quantities considered for cement, aggregates, sand, and water are 340, 1120, 820 and 181 kg/m3 respectively. Price calculation for various bacteria-carriers is represented in Table 10.

Table 10: Price calculation for various bacteria-carriers per cubic meter of concrete

Bacteria-carrier	Quantity	Unit Price (USD)	USD/m^3 of concrete	Remarks
Epoxy	20.4 kg/m^3 (6% weight of cement [11])	47.6 per 3.78 Liter [44]	205	Density =1250 kg/m^3
Ceramsite	266.56 kg/m^3 (78.4% weight of cement [10])	0.3 per kg [45]	80	-
Expanded clay particles	258.54 kg/m^3 (76.04% weight of cement [9])	150 per m^3 [46]	111	Density =350 kg/m^3 [46]
Expanded perlite	80.24 kg/m^3 (23.6% weight of cement [47])	1.5 per kg [48]	120	-
Hydrogel	17 kg/m^3 (5% weight of cement [12])	3.5 per kg [49]	60	-
Melamine	17 kg/m^3 (5% weight of cement [13])	1.2 per kg [50]	20	-
Cellulose fiber	5.5 kg/m^3 (0.5% of volume)	2.46 per kg [51]	14	Density =1100 kg/m^3

Figure 17 shows the prices in US dollars for different carrier materials required for per cubic meter of concrete.

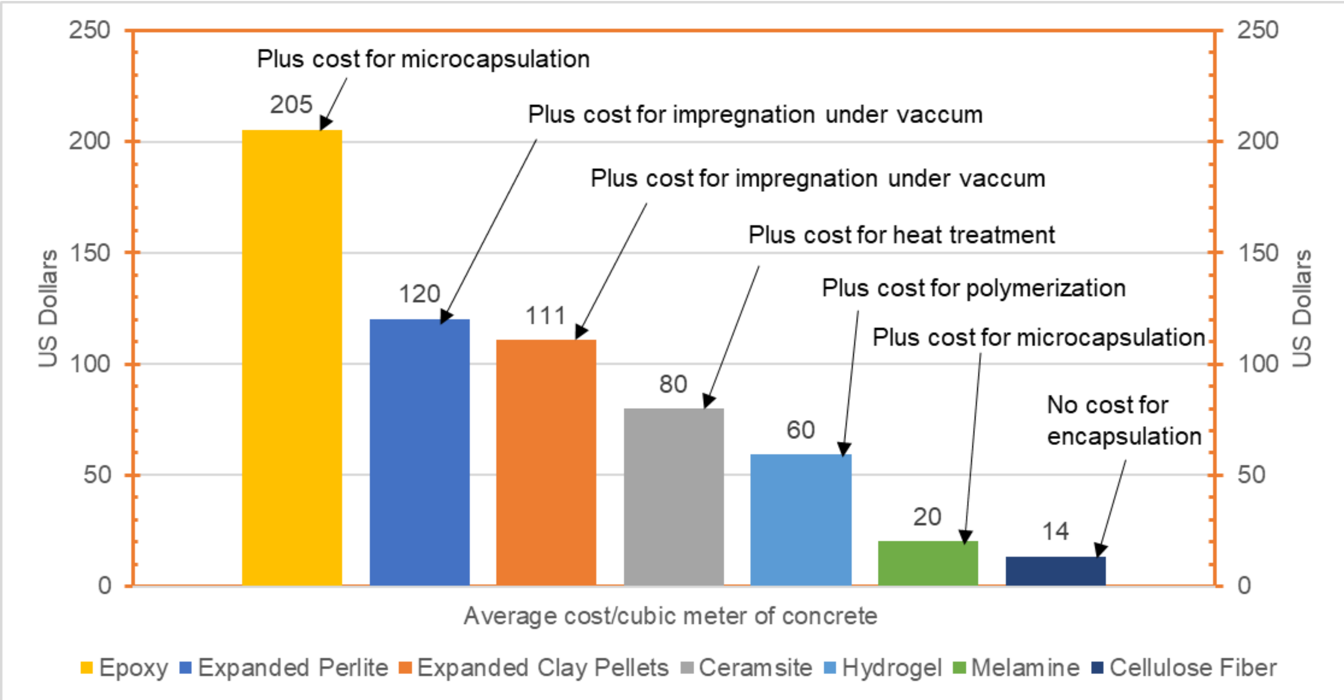

Figure 17. Material Cost in US dollars for different bacteria-carriers per m^3 of concrete

Cellulose fibers have the minimum material price as compared to other bacteria-carriers, additionally, the cost for immobilizing bacteria is zero.

After comparing different carrier materials based on immobilization technique and cost analysis, it is obvious that the method of use cellulose fibers as a carrier for bacteria is a promising option. Moreover, cellulose fiber improves the crack resistance of concrete and they are suitable to use in ready mix plant. Also, due to the high absorption rate, fibers can act as water reservoirs for promoting internal curing. Therefore, the method of using cellulose fiber as bacteria-carrier for self-healing concrete has the potential to be more widely used for large scale concrete structures.

4. Conclusions:

This paper observed the feasibility of cellulose fiber as a novel bacteria-carrier in self-healing mortar. The self-healing efficiency and compressive strength of mortar using cellulose fiber as a bacteria-carrier are compared with control and common cellulose fiber mortar. Main observations based on the experimental study employed in this project are as follows:

1. Mortars containing bacteria absorbed in cellulose fibers result in an increase in UPV with healing time for pre-cracked samples. The increase in UPV indicates the self-healing process is working well inside the crack even with a surface crack that visually does not look filled from the results of image analysis.
2. Self-healing mortar performs well when nutrients provided inside the mix for early age pre-cracked samples. However, when samples are pre-cracked at later age, better self-healing is demonstrated by samples with nutrients provided in curing water.
3. Using cellulose fiber as a bacteria-carrier (BL0.5Mxx) result in 12.04% self-healing for damaged degree between 0.1 to 0.2, when pre-cracked at 14 days of curing. However, when pre-cracked at 28 days 15.2% (B0.5Mxx) self-healing is observed, 8.23% more than control mortar for damaged degree between 0.1 to 0.2.
4. Self-healing efficiency of mortar using cellulose fiber as bacteria-carrier increases with an increase in damaged degree. However, it should be noted that there exists a damage threshold of 0.6-0.7 reported in literature beyond which self-healing efficiency may start decreasing.
5. A decrease in compressive strength is observed for all mixes containing cellulose fiber for the fiber fraction, bacteria and nutrients concentration used in this study. The mixes with different concentrations of fiber, bacteria, and nutrients are needed to be investigated for the change in compressive strength.
6. Cellulose fibers result in minimum cost as compared to other bacteria-carriers. The other characteristics like easy availability of fiber in the cracked region, simple absorption procedure, and suitability for use at a ready mix plant make cellulose fibers a promising bacteria-carrier material for small to large scale concrete construction.

Further to the finding reported in conclusion 4, authors recommend considering higher damage degree in samples in further investigations. Healing period longer than 21 days can be considered in further studies. To improve the performance (bacteria retention) of the cellulose fiber a bacteria carrier they can be coated with cement or other coating materials after absorption of the bacterial solution. In addition to the UPV tests, other destructive tests to evaluate strength recovery could be considered. SEM and XRD tests can be performed to validate self-healing performance of bacterial mortar. To study the durability and production of calcium hydroxide in bacterial mortar carbonation degree and porosity tests are also recommended.

Conflicts of Interest: The authors declare no conflict of interest.

Funding Body

This research was funded by the National Sciences and Engineering Research Council of Canada, NSERC-CRD grant.

Acknowledgments

Dr. Francis Nano and Barb Currie from Biochemistry and Microbiological department of the University of Victoria are acknowledged for their help with the growth of bacteria. The technical expertise and in-kind support provided by Mark Ryan from Solomon Ultrafiber is greatly appreciated.

Ethical Statement

We confirm that neither the manuscript nor any parts of its content are currently under consideration or published in another journal.

References:

[1] H. M. Jonkers, A. Thijssen, G. Muyzer, O. Copuroglu and E. Schlangen, "Application of bacteria as self-healing agent for the development of sustainable concrete," Ecological Engineering, vol. 36, no. 2, pp. 230-235, 2010. [CrossRef]

[2] S. Luhar and S. Gourav, "A Review Paper on Self Healing Concrete," Journal of Civil Engineering Research, vol. 2015, no. 3, pp. 53-58, 2015. [CrossRef]

[3] E. Cailleux and V. Pollet, "Investigations on the development of self-healing properties in protective coatings for concrete and repair mortars".

[4] H. Haoliang and G. Ye, "A review on self-healing in reinforced concrete structures in view of serving conditions," In 3rd International Conference on Service Life Design for Infrastructure, Zhuhai, China, pp. 1-14, 2014.

[5] H. Huang, G. Ye, C. Qian and E. Schlangen, "Self-healing in cementitious materials: Materials, methods and service conditions," Materials and Design, vol. 92, pp. 499-511, 15 2 2016. [CrossRef]

[6] J. Dick, W. De Windt, B. De Graef, H. Saveyn, P. Van Der Meeren, N. De Belie and W. Verstraete, "Bio-deposition of a calcium carbonate layer on degraded limestone by Bacillus species," Biodegradation, vol. 17, no. 4, pp. 357-367, 8 2006. [CrossRef]

[7] E. Technology, "Self-healing concrete," Engineer, vol. MAY, no. 46, pp. 39-43, 2011.

[8] J. Zhang, Y. Liu, T. Feng, M. Zhou, L. Zhao, A. Zhou and Z. Li, "Immobilizing bacteria in expanded perlite for the crack self-healing in concrete," Construction and Building Materials, vol. 148, pp. 610-617, 2017. [CrossRef]

[9] V. Wiktor and H. M. Jonkers, "Quantification of crack-healing in novel bacteria-based self-healing concrete," Cement and Concrete Composites, vol. 33, no. 7, pp. 763-770, 8 2011. [CrossRef]

[10] J. Xu, X. Wang, J. Zuo and X. Liu, "Self-Healing of Concrete Cracks by Ceramsite-Loaded Microorganisms," Advances in Materials Science and Engineering, vol. 2018, 2018. [CrossRef]

[11] B. Dong, G. Fang, W. Ding, Y. Liu, J. Zhang, N. Han and F. Xing, "Self-healing features in cementitious material with urea-formaldehyde/epoxy microcapsules," Construction and Building Materials, vol. 106, pp. 608-617, 2016. [CrossRef]

[12] J. Y. Wang, D. Snoeck, S. Van Vlierberghe, W. Verstraete and N. De Belie, "Application of hydrogel encapsulated carbonate precipitating bacteria for approaching a realistic self-healing in concrete," Construction and Building Materials, vol. 68, pp. 110-119, 2014. [CrossRef]

[13] J. Y. Wang, H. Soens, W. Verstraete and N. De Belie, "Self-healing concrete by use of microencapsulated bacterial spores," Cement and Concrete Research, vol. 56, pp. 139-152, 2014. [CrossRef]

[14] J. Wang, K. Van Tittelboom, N. De Belie and W. Verstraete, "Use of silica gel or polyurethane immobilized bacteria for self-healing concrete," Construction and Building Materials, vol. 26, no. 1, pp. 532-540, 2012. [CrossRef]

[15] K. Van Tittelboom and N. De Belie, Self-healing in cementitious materials-a review, vol. 6, 2013, pp. 2182-2217. [CrossRef]

[16] L. Souza and A. Al-Tabbaa, "Microfluidic fabrication of microcapsules tailored for self-healing in cementitious materials," Construction and Building Materials, vol. 184, pp. 713-722, 2018. [CrossRef]

[17] W. Khaliq and M. B. Ehsan, "Crack healing in concrete using various bio influenced self-healing techniques," Construction and Building Materials, vol. 102, pp. 349-357, 2016. [CrossRef]

[18] J. Y. Wang, N. De Belie and W. Verstraete, "Diatomaceous earth as a protective vehicle for bacteria applied for self-healing concrete," Journal of Industrial Microbiology and Biotechnology, vol. 39, no. 4, pp. 567-577, 4 2012. [CrossRef]

[19] R. Gupta and N. Banthia, "Correlating plastic shrinkage cracking potential of fiber reinforced cement composites with its early-age constitutive response in tension," Materials and Structures/Materiaux et Constructions, vol. 49, no. 4, pp. 1499-1509, 2016. [CrossRef]

[20] "UltraFiber Technical Bulletin UFTB #1 Plastic Shrinkage Crack Reduction," Google, [Online]. Available: https://drive.google.com/file/d/0ByWupltkC24Lc2hvWTNMVWVoc3M/view. [Accessed 14 June 2019].

[21] "5 Reasons to use Solomon UltraFiber 500," Google, [Online]. Available: https://drive.google.com/file/d/0ByWupltkC24LeUR2MWU1c2ZvOFk/view. [Accessed 14 June 2019].

[22] "UltraFiber Technical Bulletin UFTB #4 Hydration Benefit," Google, [Online]. Available: https://drive.google.com/file/d/0ByWupltkC24LekF5T2drZF9feEE/view. [Accessed 14 June 2019].

[23] "UltraFiber Technical Bulletin UFTB #3 Alkali Resistance," Google, [Online]. Available: https://drive.google.com/file/d/0ByWupltkC24LY09VZkJNcm1icGs/view. [Accessed 14 June 2019].

[24] A. Balea, E. Fuente, A. Blanco and C. Negro, "Nanocelluloses: Natural-based materials for fiber- reinforced cement composites. A critical review," Polymers, vol. 11, no. 3, 2019.

[25] "UltraFiber Technical Bulletin UFTB #7 Freeze/Thaw Durability," Google, [Online]. Available: https://drive.google.com/file/d/0ByWupltkC24LRkltZlV2OXQzZGs/view. [Accessed 14 June 2019].
[26] "UltraFiber Technical Bulletin UFTB #2 Finishability," Google, [Online]. Available: https://drive.google.com/file/d/0ByWupltkC24LS1VYRTV1ZmstR3c/view. [Accessed 14 June 2019].
[27] ASTM C150/C150M-19a, "Standard specification for Portland cement," ASTM international.
[28] B. Dileep, K. Reddy, S. Salma, P. Venkata, S. Krishna and C. K. Mounika, "Experimental Study on Bacterial Concrete," International Journal of Science Technology & Engineering, vol. 3, no. 11, pp. 171-176, 2017.
[29] "Solomon UltraFiber," [Online]. Available: http://www.ultrafiber500.com/#500. [Accessed 17 June 2019].
[30] P. Soroushian, Shahram Ravanbakhsh, "Control of plastic shrinkage cracking with specialty cellulose fibers," ACI MATERIALS JOURNAL, vol. 95, no. 4, pp. 429 - 435, 07 1998.
[31] "500 Product Information," [Online]. Available: https://www.solomoncolors.com/documents/ultrafiber/Technical%20Fiber%20Binder%20-%20500%20Specification.pdf. [Accessed 14 June 2019].
[32] "Calcium lactate, CAS No. 814-80-2," i Chemical, [Online]. Available: http://www.ichemical.com/products/814-80-2.html. [Accessed 28 June 2019].
[33] H. Singh, R. Gupta, "Strength recovery and crack healing of self-healing cement mortar containing cellulose fibers and bacteria," Proceedings of the 1st International Conference on New Horizons in Green Civil Engineering, Victoria, 2018; Abstract 30.
[34] N. Banthia, F. Majdzadeh and J. Wu, "Fiber Synergy in Hybrid Fiber Reinforced Concrete (HyFRC) in Flexure, Shear and Impact," BEFIB2012 – Fibre reinforced concrete Joaquim Barros et al. (Eds), vol. 48, pp. 91-97, 2012. [CrossRef]
[35] R. Gupta and A. Biparva, "Innovative Test Technique to Evaluate "Self-Sealing" of Concrete," Journal of Testing and Evaluation, vol. 43, no. 5, p. 20130285, 14 10 2014. [CrossRef]
[36] S. F. Selleck, E. N. Landis, M. L. Peterson, S. P. Shah and J. D. Achenbach, "Ultrasonic investigation of concrete with distributed damage," ACI Materials Journal, vol. 95, no. 1, pp. 27-36, 1998. [CrossRef]
[37] N. F. Ariffin, M. W. Hussin, A. R. Mohd Sam, H. Seung Lee, N. H. Nur, N. H. Abdul Shukor Lim and M. Samadi, "Mechanical properties and self-healing mechanism of epoxy mortar," Jurnal Teknologi, vol. 77, no. 12, pp. 37-44, 2015. [CrossRef]
[38] M. A. K. Bahrin, M. F. Othman, N. H. N. Azi and M. F. Talib, " Performance of Epoxy Resin as Self-Healing Agent," Jurnal Teknologi (Sciences & Engineering), vol. 78, no. 6-13, pp. 137 - 143, 2016. [CrossRef]
[39] M. Sarkar, T. Chowdhury, B. Chattopadhyay, R. Gachhui and S. Mandal, "Autonomous bioremediation of a microbial protein (bioremediase) in Pozzolana cementitious composite," Journal of Materials Science, vol. 49, no. 13, pp. 4461-4468, 2014. [CrossRef]
[40] ASTM C597-16, "Standard Test Method for Pulse Velocity Through Concrete," ASTM international.
[41] ASTM C579-18, "Standard test method for compressive strength of chemical-resistant mortars, grouts, monolithic surfacings, and polymer Concretes".," ASTM international.
[42] W. Zhong and W. Yao, "Influence of damage degree on self-healing of concrete," Construction and Building Materials, vol. 22, no. 6, pp. 1137-1142, 2008. [CrossRef]
[43] K. Vijay and M. Murmu, "Effect of calcium lactate on compressive strength and self-healing of cracks in microbial concrete," Frontiers of Structural and Civil Engineering, vol. 13, no. 3, pp. 515-525, 2018. [CrossRef]
[44] "EPOXY Resin 1 Gal Kit, General Purpose," [Online]. Available: https://www.amazon.com/dp/B01IU9XYVE/ref=psdc_13399741_t1_B00NLPCA5Y. [Accessed 09 July 2019].
[45] "Water Treatment Ceramsite With Factory Price," [Online]. Available: https://www.alibaba.com/product-detail/Water-Treatment-Ceramsite-With-Factory-Price_60808255387.html?spm=a2700.7724857.normalList.34.430a2a99hQD3Vz. [Accessed 09 July 2019].
[46] "Hydroponic Growing Media Lightweight Expanded Clay Pebbles Pellets," [Online]. Available: https://www.alibaba.com/product-detail/Hydroponic-Growing-Media-Lightweight-Expanded-Clay_60777685703.html?spm=a2700.7724857.normalList.32.1d04daact4Kt9a. [Accessed 09 July 2019].
[47] M. Alazhari, T. Sharma, A. Heath, R. Cooper and K. Paine, "Application of expanded perlite encapsulated bacteria and growth media for self-healing concrete," Construction and Building Materials, vol. 160, no. January, pp. 610-619, 2018. [CrossRef]
[48] "Lightweight Concrete Expanded Concrete Perlite For Sale," [Online]. Available: https://www.alibaba.com/product-detail/Lightweight-Concrete-Expanded-Concrete-Perlite-For_60775442681.html?spm=a2700.7724857.normalList.1.24b96118i9wdRG. [Accessed 09 July 2019].
[49] "sap hydrogel for agriculture," [Online]. Available: https://www.alibaba.com/product-detail/sap-hydrogel-for-agriculture_60781845485.html?spm=a2700.7724857.normalList.12.3c3658eeosYjC5&s=p. [Accessed 09 July 2019].
[50] "Factory supply white powder Melamine 99.8%," [Online]. Available: https://www.alibaba.com/product-detail/Factory-supply-white-powder-Melamine-99_60806647259.html?spm=a2700.7724838.2017115.11.64bc6efbN9haMr&s=p. [Accessed 09 July 2019].

[51] "Cellulose fiber," [Online]. Available: https://www.alibaba.com/product-detail/Cellulose-fiber_1529438436.html?spm=a2700.7724838.2017115.23.24c76d86iHHDcv. [Accessed 09 July 2019].